

Ni-CeO₂ Cermets Synthesis by Solid State Sintering of Ni/CeO₂ Multilayer

Aleksandras ILJINAS*, Saulius BURINSKAS

Department of Physics, Kaunas University of Technology, Studentų 50, LT-51368 Kaunas, Lithuania

crossref <http://dx.doi.org/10.5755/j01.ms.19.4.3037>

Received 10 December 2012; accepted 08 July 2013

Nickel and gadolinium doped cerium oxide (GDC) cermet is intensively investigated for an application as an anode material for solid oxide fuel cells based on various electrolytes. The purpose of the present investigation is to analyze morphology, microstructure, and optical properties of deposited and annealed for one hour in the temperatures from 500 °C to 900 °C Ni/CeO₂ multilayer thin films deposited by sputtering. The crystallographic structure of thin films was investigated by X-ray diffraction. The morphology of the film cross-section was investigated with scanning electron microscope. The elemental analysis of samples was investigated by energy-dispersive X-ray spectroscopy. The fitting of the optical reflectance data was made using Abeles matrix method that is used for the design of interference coatings.

The film cross-section of the post-annealed samples consisted of four layers. The first CeO₂ layer (on Si) had the same fine columnar structure with no features of Ni intermixing. The part of Ni (middle-layer) after annealing was converted to NiO with grain size exceeding 100 nm. The CeO₂ layer deposited on Ni was divided into two layers. Lower layer had small grains not exceeding 25 nm and consisting of NiO and CeO₂ mixture. Upper layer consisted of CeO₂ columns with approximate thickness of 50 nm. Ni sample annealed at 600 °C was fully oxidized. The NiO thickness and refraction index were almost steady after annealing in various temperatures. The approximation of experimental reflectance data was successful only for the samples with one transparent homogeneous layer. The reflectance of the Ni/CeO₂ samples annealed at intermediate temperatures could not be fitted using one-layer or three-layer model. That may show that a simplified model could not be implemented. The real system has complicated distribution of refraction index.

Keywords: anode materials for solid oxide fuel cells, solid state reactions, sputtering, and reflectance.

1. INTRODUCTION

Doped cerium oxide is intensively investigated for an application in the intermediate temperature solid oxide fuel cells (SOFC) [1]. The higher ionic conductivity of gadolinium doped ceria comparing it to the conventional electrolyte material of yttria-stabilized zirconia (YSZ) makes it very attractive material, because lower operation (<800 °C) temperature allows to use cheaper SOFC components, overcome fast ageing, and other problems [2]. Ni and Gd doped cerium oxide (GDC) cermet is intensively investigated for an application as an anode material for solid oxide fuel cells based on various electrolytes [1]. Ni-GDC cermet material is reported at one of the best choices for this application because it has low anode over potential, high electrical conductivity, strong electrochemical activity and stability at high temperature [3–5].

One problem arising with conventional sintering technology, which is used to form cermets via solid state reactions, is the requirement of the temperatures exceeding 1300 °C. The rather high grain growth rates at those temperatures result in large grains and therefore poor mechanical stability [6] and weak electrochemical activity [7]. Many attempts have been made to decrease the sintering temperature of Gd doped ceria, including the use of nano-sized powder produced by various wet-chemical methods [8, 9], ball milling [10] and the addition of sintering aids, such like Bi₂O₃ [11], Co₃O₄ [12]. There are no analogous studies in the literature about Ni-CeO₂ system.

Solid state reaction for multilayer Ni and CeO₂ films could be used to lower sintering temperature, since this method gives the possibility to deposit thin films with bilayer period smaller than the diffusion length of the atoms and therefore does not require long heating at high temperature.

The sputter deposition method that was chosen for the deposition of thin films in this work is an ideal candidate since the films are deposited in the plasma environment. Thin films are dense, nanocrystalline and may include many point defects due to ion bombardment from plasma during film growth [13]. Enhanced diffusion and fast mixing of the deposited multilayer is expected at the range of intermediate temperatures [14].

There is not enough information about possibility to form Ni-CeO₂ cermets by solid state reactions of Ni/CeO₂ multilayer thin film; therefore, the purpose of the present investigation is to analyze morphology, microstructure and optical properties of as deposited and annealed Ni/CeO₂ multilayer thin films deposited by sputtering.

2. EXPERIMENTAL DETAILS

CeO₂ thin films were deposited by reactive direct current magnetron sputtering in Ar + O₂ atmosphere, while Ni layers were deposited by DC diode sputtering in Ar atmosphere. The substrates were Si (111) wafers. The detailed conditions of the experiment are presented in Table 1.

After the deposition the samples were annealed for one hour at the temperatures from 500 °C to 900 °C. The heating and cooling rates were less than 10 °C degrees per minute in all annealing steps. The atmosphere was static air.

*Corresponding author. Tel.: +370-615-23668; fax: +370-37-456472.
E-mail address: aleksandras.iljinas@ktu.lt (A. Iljinas)

The crystallographic structure of thin films was investigated by X-ray diffraction (XRD) studies using Bruker D8 Discover diffractometer with monochromatic CuK_α radiation ($\lambda = 0.15418 \text{ nm}$).

The morphology of the film cross-section was investigated with scanning electron microscope (SEM) FEI Quanta 200F in secondary electron mode. The sample was broken after cooling in liquid nitrogen. The elemental analysis of samples was investigated by energy-dispersive X-ray spectroscopy (EDX) method using cross-section scan.

Table 1. Experimental conditions

Parameter	Ni	CeO ₂
Residual gas pressure, Pa	5.0·10 ⁻³	
Discharge atmosphere	Ar	Ar + O ₂
Working pressure, Pa	5.0	0.6
Oxygen partial pressure, Pa	1.1·10 ⁻³	1.1·10 ⁻¹
Discharge voltage, V	2200	250
Discharge current density, mA/cm ²	1.6	23.6
Temperature of the substrate	ambient	

The evaluation of layers intermixing was performed by measuring the reflection spectra of Ni/CeO₂ bilayers deposited on Si substrates and annealed for one hour at various temperatures. The spectra were collected using an Ocean Optics spectrophotometer equipped with a CCD detector. The fitting of the experimental data was made using Abeles matrix method that is used for the design of interference coatings [16]. At normal to the surface light incidence the characteristic matrix of the j -layer with thickness d_j and index of refraction n_j is:

$$M_j = \begin{pmatrix} \cos\left(\frac{2\pi}{\lambda}n_jd_j\right) & \frac{i}{n_j}\sin\left(\frac{2\pi}{\lambda}n_jd_j\right) \\ i\cdot n_j\sin\left(\frac{2\pi}{\lambda}n_jd_j\right) & \cos\left(\frac{2\pi}{\lambda}n_jd_j\right) \end{pmatrix}. \quad (1)$$

The product of characteristic matrices of all layers is:

$$M = M_m \cdot M_{m-1} \dots M_1 = \begin{pmatrix} m_{11} & m_{12} \\ m_{21} & m_{22} \end{pmatrix}. \quad (2)$$

The reflection coefficient R is calculated according the equation:

$$R = \left| \frac{n_a \cdot m_{11} - n_s \cdot m_{22} + n_a \cdot n_s \cdot m_{12} - m_{21}}{n_a \cdot m_{11} + n_s \cdot m_{22} + n_a \cdot n_s \cdot m_{12} + m_{21}} \right|^2, \quad (3)$$

where n_s and n_a are the substrate (Si or Ni in our case) and ambient (air) indexes of refraction respectively. The index of refraction of intermixed layer was calculated according M. Garnet "Effective medium" theory neglecting the extinction coefficient k [17]:

$$\frac{1}{n_{eff}^2} = (1-q)\frac{1}{n_{ceO2}^2} + q\frac{1}{n_{NiO}^2}. \quad (4)$$

where q denotes the fraction of nickel oxide in the layer.

3. RESULTS AND DISCUSSION

The diffusion profile simulations were made using model of 100 nm Ni layer-marker embed in CeO₂ matrix.

Since the data about the diffusion in Ni-CeO₂ system were not available, data of similar NiO-La₂O₃ system were used [18].

The diffusion profile of $d_0 = 100 \text{ nm}$ thickness layer-marker annealed in various temperatures T for $t = 3600 \text{ s}$ (1 hour) was calculated according the equations [19]:

$$C(x,t,T) = \frac{C_0}{2} \left(\operatorname{erf}\left(\frac{0.5d_0 - x}{\sqrt{4 \cdot D(T) \cdot t}}\right) + \operatorname{erf}\left(\frac{0.5d_0 + x}{\sqrt{4 \cdot D(T) \cdot t}}\right) \right); \quad (5)$$

$$D(T) = D_0 e^{\frac{-E_a}{RT}}, \quad (6)$$

where $C_0 = 1$ is the primary concentration, $E_a = 237.5 \text{ kJ/mol}$ is Ni self-diffusion activation energy, $D_0 = 2.01 \cdot 10^{-4} \text{ cm}^2\text{s}^{-1}$ is pre-exponential factor, $R = 8.31 \text{ J}\cdot\text{K}^{-1}\text{mol}^{-1}$ is the ideal gas constant.

The results of the simulation are presented in Fig 1. The multilayer period below 100 nm is thin enough to mix the layers in the temperatures exceeding 800 °C (Fig 1).

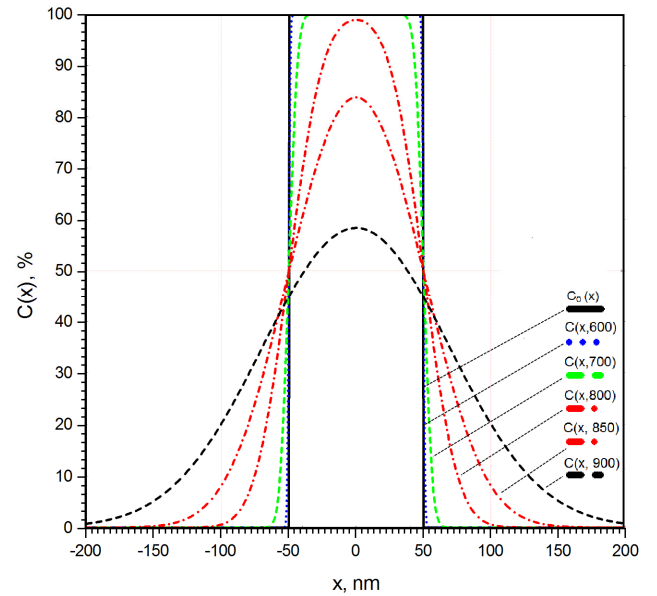


Fig. 1. The diffusion profile of Ni layer-marker annealed in various temperatures for one hour

Fig. 2 and Fig. 3 shows the cross-sectional SEM images of CeO₂/Ni/CeO₂ multilayer thin films as deposited and annealed at 600 °C. Before annealing the film cross-section consists of three layers with different morphology (Fig. 2). CeO₂ layer on the Si substrate had fine columnar structure. Ni (middle-layer) and CeO₂ layer on the top of the Ni layer have dense structure. Upper CeO₂ layer has no visible features of columnar structure. The morphology of the system in the post-annealed sample is different. As it can be seen from Fig. 3, the film cross-section consists of four layers. The first CeO₂ layer (on Si) has the same fine columnar structure with no Ni intermixing features. The part of Ni middle-layer after annealing was converted to NiO with grain size exceeding 100 nm. The CeO₂ layer deposited on Ni was divided into two layers, lower has small grains do not exceeding 25 nm and consist of NiO and CeO₂, mixture. Upper layer consists of CeO₂ columns with approximate thickness of 50 nm.

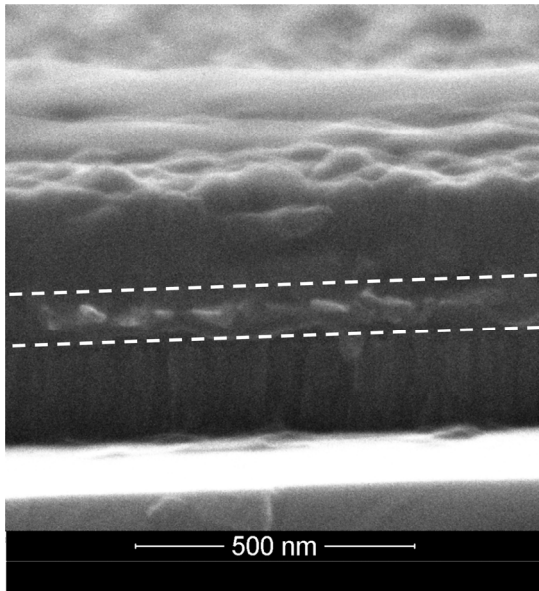


Fig. 2. SEM cross-section image of as deposited $\text{CeO}_2/\text{Ni}/\text{CeO}_2$ multilayer film on Si substrate

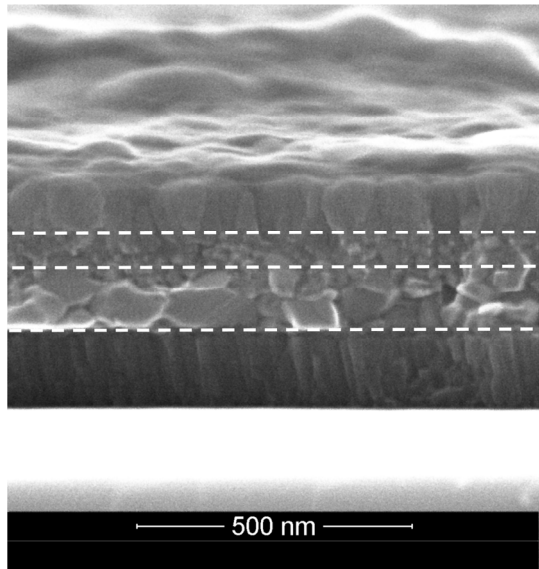


Fig. 3. SEM cross-section image of annealed at 600°C $\text{CeO}_2/\text{Ni}/\text{CeO}_2$ multilayer film on Si substrate

The EDX line profile scan was made to confirm the mixing of layers (Fig. 4). The standard EDX scan resolution is too low to be used for the characterization of multilayer thin films with bilayer thickness below $1\ \mu\text{m}$, because the excited volume exceeds the film thickness. Despite this fact, the scan data support the assumption made from the SEM images about mixing between NiO and upper CeO_2 layer. The maximum of $\text{Ni}_{\text{K}\alpha}$ profile not only decreases after annealing, but also becomes asymmetric (Fig. 4).

It is well known that Ni thin film can be fully oxidized at the temperature exceeding 350°C . The structural analysis made by X-ray diffraction (Fig. 5) confirmed that after annealing the sample at 600°C temperature Ni was fully oxidized. Before annealing XRD pattern consists of the peaks that belongs to fcc- CeO_2 (PDF Card No. 01-081-0792) and fcc-Ni (PDF Card No. 00-004-0850), while after

annealing fcc-Ni peaks disappeared and were replaced by fcc-NiO peaks (PDF Card No. 00-047-1049).

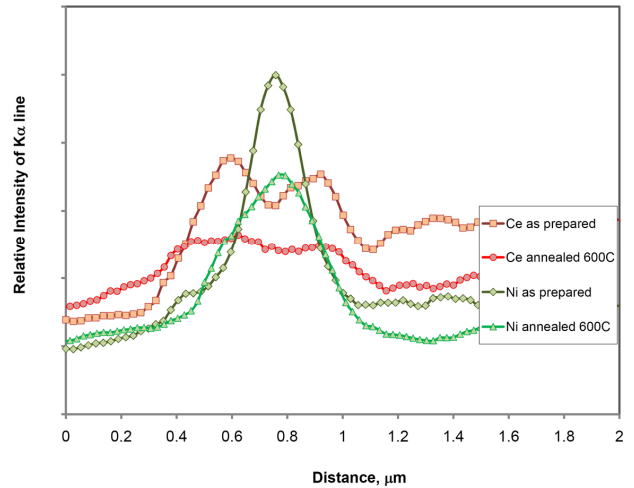


Fig. 4. The results of EDX elemental profile scan of the sample cross-section image of as prepared and annealed at 600°C $\text{CeO}_2/\text{Ni}/\text{CeO}_2$ multilayer film on Si substrate

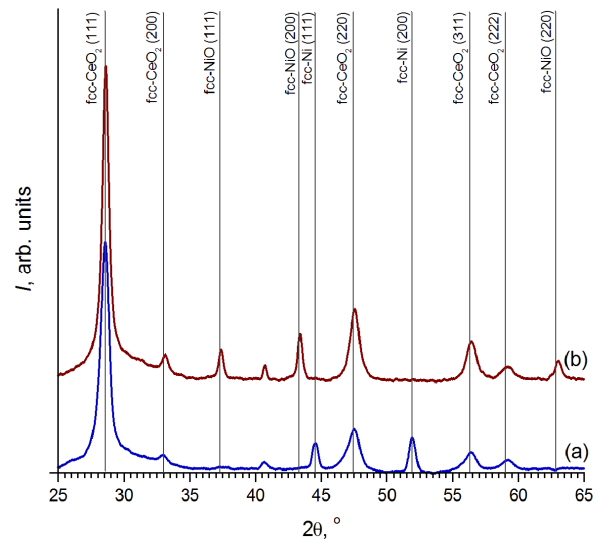


Fig. 5. XRD patterns of a) as deposited and b) annealed at 600°C $\text{CeO}_2/\text{Ni}/\text{CeO}_2$ multilayer films produced on the Si substrate

Optical characterization of the films was made using reflectance measurement data. The reflectance spectra of the Ni/CeO_2 bilayer samples are presented in Fig. 6. The character of the spectra does not change if the annealing temperature is higher than 700°C (Fig. 6), because the oxidation of Ni becomes rapid already in the temperatures exceeding 350°C [20]. The reflectance of CeO_2 uncoated Ni samples deposited and annealed at the same conditions was measured in order to confirm this assumption (Fig. 7). As it can be seen in the Fig. 7, the NiO thickness and index of refraction do not changes a lot upon annealing at different temperatures, because the peaks of the reflectance curves remain almost in the same positions.

The decrease of reflectance maximum of CeO_2 coated Ni/NiO thin films from $R_{\text{m,as.prep.}} = 62.7\%$ to $R_{\text{m,900}} = 12.5\%$ is related to scattering due to increased roughness of the sample surface.

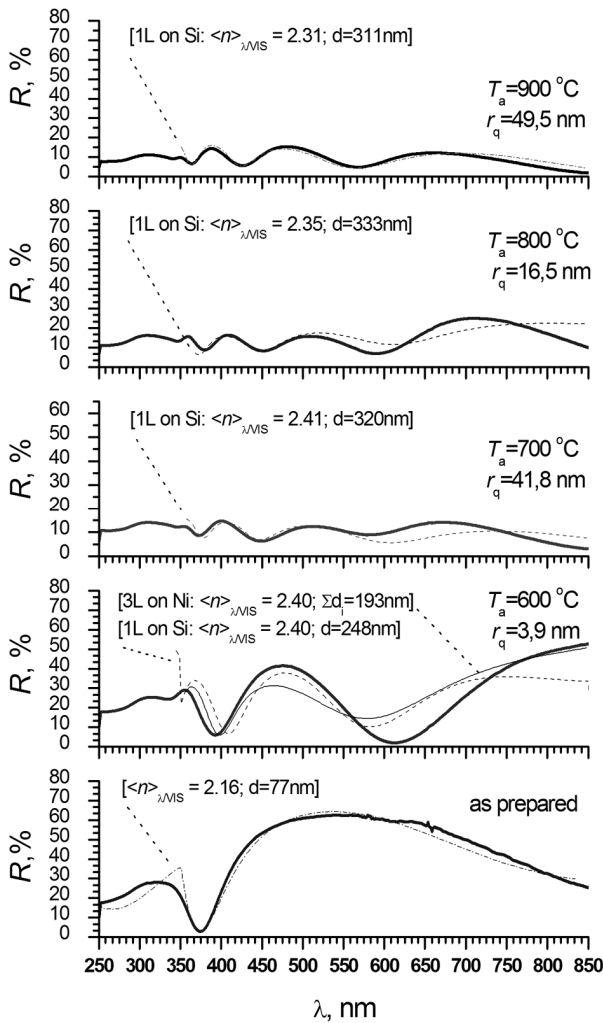


Fig. 6. Reflectance spectra of the deposited and annealed Ni/CeO₂ bilayer films deposited on Si substrates

The mean square roughness r_q of the surface was measured with surface profilometer to confirm this assumption (the results are indicated in Fig. 6). The substantial change of the oscillation period of reflectance curves of CeO₂ coated Ni samples shows that after annealing the sample at 600 °C, the thickness of transparent layer increased, but Ni was not fully oxidized until annealing at 700 °C. The further changes after annealing at higher temperatures may be attributed in the small changes of index of refraction of the layers. That may show that the mixing process takes place in the film. The approximation of experimental reflectance data was successful only for the samples with one transparent homogeneous layer (as prepared Ni/CeO₂, Ni/CeO₂ and Ni films annealed at 900 °C). The reflectance of the Ni/CeO₂ samples annealed at intermediate temperatures could not be fitted using one-layer or three-layer model. That may show that simplified model could not be implemented since the real system. The real system has complicated distribution of refraction index.

4. CONCLUSION

The film cross-section of the post-annealed samples consists of four layers. The first CeO₂ layer has columnar

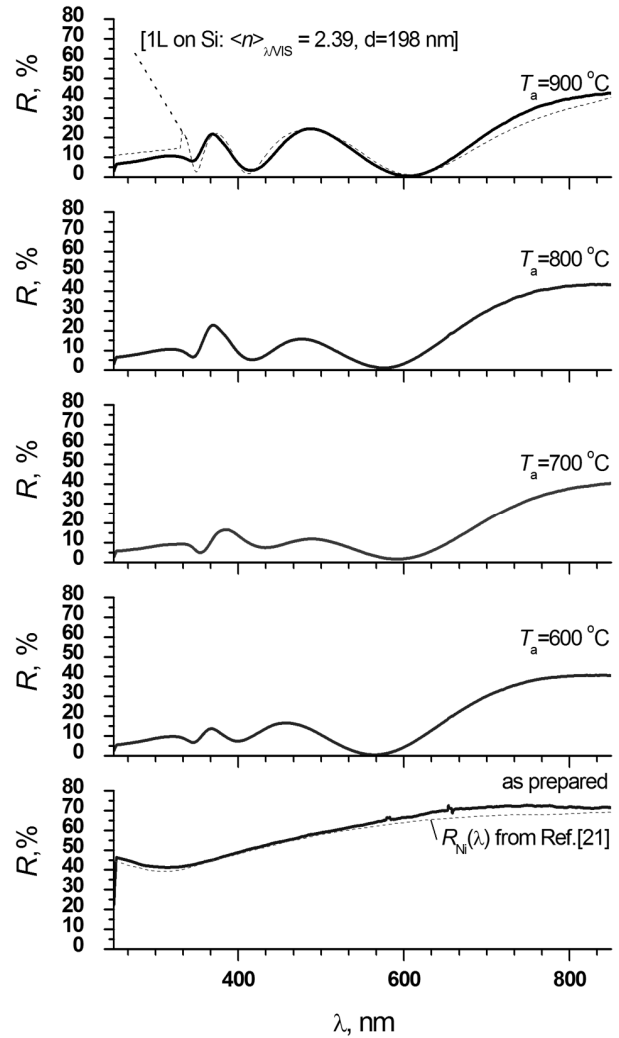


Fig. 7. Reflectance spectra of the as deposited and annealed Ni thin films deposited on Si substrates

structure with no Ni intermixing features. The part of Ni layer after annealing converted to NiO with grain size exceeding 100 nm. The CeO₂ layer deposited on Ni was divided into two layers. Lower layer has small grains that do not exceed 25 nm. This layer consists of NiO and CeO₂ mixture. Upper layer consists of CeO₂ columns with approximate thickness of 50 nm. The investigation of reflectance of the annealed Ni/CeO₂ bilayer thin film samples showed that NiO/CeO₂ layers mixing can be achieved at the temperatures lower than 900 °C, but longer than one hour time or smaller bilayer period than 70 nm is needed to achieve an uniform distribution of the concentration. The approximation of experimental reflectance data was successful only for the samples with one transparent homogeneous layer. The reflectance of the Ni/CeO₂ samples annealed at intermediate temperatures could not be fitted using one-layer or three-layer model, what show that simplified model could not be implemented. The real system has complicated distribution of refraction index.

Acknowledgments

The authors would like to thank M. Lelis from Lithuanian Energy Institute for performing the XRD measurements.

REFERENCES

1. **Steele, B. C. H.** Materials for IT-SOFC Stacks: 35 Years R&D: the Inevitability of Gradualness? *Solid State Ionics* 134 (1–2) 2000: pp. 3–20.
2. **Briois, P., Billard, A.** A Comparison of Electrical Properties of Sputter-Deposited Electrolyte Coatings Dedicated to Intermediate Temperature Solid Oxide Fuel Cells *Surface and Coatings Technology* 201 (3–4) 2006: pp. 1328–1334.
3. **Gil, V., Moure, C., Tartaj, J.** Sinter Ability, Microstructures and Electrical Properties of Ni/Gd-doped Ceria Cermets Used as Anode Materials for SOFCs *Journal of the European Ceramic Society* 27 2007: pp. 4205–4209. <http://dx.doi.org/10.1016/j.jeurceramsoc.2007.02.119>
4. **Datta, P., Majewski, P., Aldinger, F.** Synthesis and Reactivity Study of Gadolinia Doped Ceria-nickel: A Potential Anode Material for Solid Oxide Fuel Cell *Journal of Alloys and Compounds* 455 (1–2) 2008: pp. 454–460.
5. **Gil, V., Tartaj, J., Moure, C.** Chemical and Thermomechanical Compatibility between Ni-GDC Anode and Electrolytes Based on Ceria *Ceramics International* 35 (2) 2009: pp. 839–846.
6. **Hui, Sh. R., Roller, J., Yick, S., Zhang, X., Deces-Petit, C., Xie, Y., Maric, R., Ghosh, D.** A Brief Review of the Ionic Conductivity Enhancement for Selected Oxide Electrolytes *Journal of Power Sources* 172 (2) 2007: pp. 493–502.
7. **Gil, V., Larrea, A., Merino, R. I., Orera, V. M.** Redox Behaviour of Gd-doped Ceria-nickel Oxide Composites *Journal of Power Sources* 192 (1) 2009: pp. 180–184.
8. **Dikmen, S., Shuka, P., Greenblatt, M., Gocmez, H.** Hydrothermal Synthesis and Properties of $\text{Ce}_{1-x}\text{Gd}_x\text{O}_{2-\Delta}$ Solid Solutions *Solid State Sciences* 4 (5) 2002: pp. 585–590. [http://dx.doi.org/10.1016/S1293-2558\(02\)01301-8](http://dx.doi.org/10.1016/S1293-2558(02)01301-8)
9. **Yashiro, K., Onuma, S., Kaimai, A., Nigara, Y., Kawada, T., Mizusaki, J., Kawamura, K., Horita, T., Yokokawa, H.** Mass Transport Properties of $\text{Ce}_{0.9}\text{Gd}_{0.1}\text{O}_{2-\Delta}$ at the Surface and in the Bulk *Solid State Ionics* 152–153 2002: pp. 469–476.
10. **Jung, W.-S., Park, H. S., Kang, Y. J., Yoon, D.-H.** Lowering the Sintering Temperature of Gd-doped Ceria by Mechanochemical Activation *Ceramics International* 36 (1) 2010: pp. 371–374.
11. **Gil, V., Tartaj, J., Moure, C., Duran, P.** Sintering, Microstructural Development, and Electrical Properties of Gadolinia-doped Ceria Electrolyte with Bismuth Oxides as a Sintering Aid *Journal of the European Ceramic Society* 26 (15) 2006: pp. 3161–3171.
12. **Kleinlogel, C., Gauckler, L. J.** Sintering and Properties of Nanosized Ceria Solid Solutions *Solid State Ionics* 135 (1–4) 2000: pp. 567–573.
13. **Musila, J., Baroch, P., Vlcek, J., Nam, K. H., Han, J. G.** Reactive Magnetron Sputtering of Thin Films: Present Status and Trends *Thin Solid Films* 475 (1–2) 2005: pp. 208–218.
14. **Bracht, H.** Diffusion Mediated by Doping and Radiation-induced Point Defects *Physica B* 376–377 2006: pp. 11–18.
15. **Mansilla, C.** Structure, Microstructure and Optical Properties of Cerium Oxide Thin Films Prepared by Electron Beam Evaporation Assisted with Ion Beams *Solid State Sciences* 11 (8) 2009: pp. 1456–1464.
16. **Kaiser, N., Pulker, H. K.** (Eds.), *Optical Interference Coatings*. Springer, Berlin, 2003: pp. 82–84. <http://dx.doi.org/10.1007/978-3-540-36386-6>
17. **Guezmir, N., Ouerfelli, J., Belgacem, S.** Optical Properties of Sprayed CuIn_2 Thin Layers *Materials Chemistry and Physics* 96 (1) 2006: pp. 116–123. <http://dx.doi.org/10.1016/j.matchemphys.2005.06.059>
18. **Čebašek, N., Haugsrud, R., Smith, J. B., Norby, T.** Determination of Ni_2^+ Self Diffusion Coefficient in $\text{La}_2\text{NiO}_{4+d}$ by the Solid State Reaction Method *214th ECS Meeting*, © *The Electrochemical Society*, Abstract #1774, 2008, MA 2008-02 / D5 High Temperature Corrosion and Materials Chemistry.
19. **Mehrer, H.** Diffusion in Solids. Fundamentals, Methods, Materials, Diffusion-Controlled Processes *Springer Series in Solid-State Sciences* 155 2007: pp. 43–44.
20. **Courtade, L., Turquat, Ch., Muller, Ch., Lisoni, J. G., Goux, L., Wouters, D. J., Goguenheim, D., Roussel, P., Ortega, L.** Oxidation Kinetics of Ni Metallic Films: Formation of Nio-Based Resistive Switching Structures *Thin Solid Films* 516 2008: pp. 4083–4092. <http://dx.doi.org/10.1016/j.tsf.2007.09.050>
21. **Weber, M. J.** (Ed.) *Handbook of Optical Materials*. CRC Press, 2003: pp. 340–341.